Supplementary Information for

Reliable Food and Water Resources of Late Pleistocene-to-Holocene Lesotho, Southern Africa, Facilitated Human Upland Habitation.

Robert Patalano*, Charles Arthur, William Christopher Carleton, Sam Challis, Genevieve Dewar, Kasun Gayantha, Gerd Gleixner. Jana Ilgner, Mary Lucas, Sara Marzo, Rethabile Mokhachane, Kyra Pazan, Diana Spurite, Mike W. Morley, Adrian Parker, Peter Mitchell, Brian A. Stewart, and Patrick Roberts*

*Email: patalano@bryant.edu, roberts@shh.mpg.de

This PDF file includes:

Supplementary Discussion
Figures S1 to S5
Table S1
Replication for Age-Depth Model of Ha Makotoko and Figure S6
SI References

Other supplementary materials for this manuscript include the following:

Dataset 1

Supplementary Information Text

SI Discussion

Plant Wax Biomarkers. The ubiquitous, well-preserved nature of lipid biomarkers allows for their distribution to differentiate between sources of production[1,2]. Generally, short-chain homologues (C_{17}-C_{21} *n*-alkanes) characterize aquatic algae[3], mid-chain homologues (C_{21}-C_{25} *n*-alkanes) characterize submerged and floating aquatic macrophytes[4-6], and long-chain homologues (C_{27}-C_{35} *n*-alkanes) characterize terrestrial vegetation[7]. All Ha Makotoko samples were dominated by long-chain compounds. The C_{31} *n*-alkane is the most abundant compound in all 16 samples, and of these, eight samples have C_{31} followed by C_{33}, C_{29}, C_{35}, and C_{27}, four samples have a relative abundance distribution of C_{31}, C_{33}, C_{29}, C_{27}, and C_{35}, three samples have C_{31}, C_{29}, C_{33}, C_{27}, and C_{35}, and one sample has C_{31}, C_{29}, C_{27}, C_{33}, and C_{35} (Fig S3). Although these distributions are not diagnostic of the specific plant types that produced them, grasses tend to produce higher chains (C_{33}, C_{35}) than co-occurring shrubs or trees[8]. Furthermore, the relative abundance of specific *n*-alkanes can correlate with temperature and aridity[9-14], so caution must be taken when using chain-length distributions as a diagnostic biomarker for plant ecological composition.

Plant Wax Isotope Ratios. Compound-specific isotope analyses is necessary to make inferences on plant community composition and the main sources of plant waxes to depositional environments. The *n*-alkane $\delta^{13}C$ values provide information on plant type and photosynthetic pathway[15], the intensity and duration of sunlight[16], canopy structure and wax production[17], plant taxonomy[18], and the total concentration of atmospheric CO_2[19]. In terrestrial contexts, variations in $\delta^{13}C$ are influenced by biological differences in photosynthetic pathways and the degree to which different plant types discriminate against ^{13}C during carbon fixation, which leads to distinct and, for the most part, non-overlapping values between C_3 and C_4 plants[15,20,21]. C_3 plants typically have bulk leaf $\delta^{13}C$ ranging between -20 to -35 ‰. C_4 plants, which do not discriminate against the heavier ^{13}C to such a large degree, have values that span from -7 to -15 ‰[20]. Plant wax *n*-alkanes are further depleted from their bulk values by about -5 ‰ to -7 ‰ for C_3 vegetation and -8 ‰ to -10 ‰ for C_4 types. Therefore, depending on plant ecological lifeform, water availability, canopy structure, and other factors, C_3 terrestrial plant *n*-alkane values can range from -25 ‰ to -42 ‰ (average -35 ‰), while C_4 plants range from about -14 ‰ to -26 ‰ (average -21 ‰)[15,22-25]. However, this can be complicated by some emergent plants, such as *Typha angustifolia*, having *n*-alkane distributions that also maximize at C_{31}[26]. To complicate matters further, *Typha* has a C_4 isotopic signal with values around -21 ‰[26], and though this value is easily distinguished from C_3 terrestrial plant *n*-alkane $\delta^{13}C$, *Typha* wax deposits in paleo-archives could be misinterpreted as a C_4 plant signal.

Increases in the relative abundance of *Typha* have been documented in the Holocene in southern Africa. Both phytolith results and $\delta^{13}C$ values indicate an expansion of *Typha* during locally warm and humid conditions in coastal Mpondoland during the early Holocene[27]. There is no evidence in the phytolith assemblage for the expansion of *Typha* during the Holocene along the Phuthiatsana River, however (Parker et al., In prep.). Through our data, we therefore infer an increase in C_4 grasses with warm and humid conditions in the later Holocene at Ha Makotoko (see main manuscript).

Carbon isotope ratios are also indicators of plant water-use efficiency (WUE), the ratio of the rate of carbon assimilation (photosynthesis) to the rate of water loss (transpiration) in plants[21,28]. In terms of carbon-13 isotope values, plants with greater WUE are proportionally enriched in ^{13}C than well-watered analogs[18,21,29]. WUE is a function of plant type and physiological mechanism, and depends on such climatic factors as humidity, sunlight exposure, and temperature[14,28,30]. Plants with higher WUE have also been shown to synthesize plant waxes with lower δD (c.f. [25,31]), due to reduced transpiration rates during photosynthesis[28].

Ultimately, source water hydrogen is the primary signal recorded in the δD values of *n*-alkanes and other plan wax biomarkers[25,32-35]. Although variability exists in the δD of plant waxes in regard to source water[14,18,34,36,37], regional meteoric water δD is the primary control on plant wax signatures[25,32,38]. In Lesotho, precipitation δD is influenced by the *rainout* process[39,40] with ^{2}H-depleted moisture falling during the rainy months (Fig S4). However, as the wettest months are also the warmest, heightened temperature and evapotranspiration can also influence the δD of plant wax biomarkers. Lesotho receives most (~80 %) of their mean annual precipitation (MAP) between October and March, sourced from the Indian Ocean and brought by tropical easterlies. This is referred to as the summer rainfall zone (SRZ).

Plant Type Distribution and Ecology. In general, C_4 plants will outcompete C_3 analogs under conditions of aridity coupled with intense irradiation, high temperatures, fire history, or low CO_2 concentrations[21,41,42]. On the other hand, water availability is the dominant factor dictating forest and woodland development in southern Africa, as woody vegetation composition and structure is a function of amount of precipitation, evapotranspiration, availability of groundwater, soil structure, and seasonality of precipitation[43]. However, in areas with high geomorphological and hydrological variability, topography-induced micro-climates and environments can form on small spatial scales, such as in stream channels, where severe temperature inversions in deeply incised valleys can enhance/diminish growing conditions for certain plant types (Patalano et al., In prep). For example, woody plants notably grow within stream channels in Lesotho warmer valleys.

Today, Lesotho is covered by a mosaic of grassland, with the number of vegetation types reflecting the severity of temperature and precipitation seasonality[43]. The Drakensberg Grassland is the dominant bioregion of central and eastern Lesotho while the Mesic Highveld Grassland bioregion, in which Ha Makotoko is found, extends throughout western and northwestern Lesotho and in major river valleys (Fig. 1B, main manuscript)[43]. Due to its high elevation, the Drakensberg Grassland bioregion is dominated by C_3 grasses, whereas the Mesic Highveld Grassland bioregion has a high number of C_3 and C_4 vegetation types with both greater grass and herb diversity, especially in undulating terrain and along streams and rivers that drain the foothills of the Drakensberg. Tall and often dense, broad-leaved shrubland is common in areas with abundant rainfall or surface water, specifically within stream valleys.

Generally, from an ecological sense, the Maloti-Drakensberg can be separated into Montane, Subalpine, and Alpine vegetation altitudinal zones, with transitions between zones occurring lower or higher on slopes according to aspect[43-45]. *Themeda triandra* (C_4 grass) tends to be more important at the lower and middle elevations while *Festuca caprina* (C_3 grass) dominates at higher altitudes, although there is considerable altitudinal overlap between these species[46]. The medium-tall grass *Merxmuellera macowanii* occurs along water courses and drainage lines, like in the Phuthiatsana Gorge, but herb species in the Asteraceae family increase alpha diversity considerably.

In Lesotho, temperature variations linked to altitude and aspect produce particularly sharp gradients of C_4 to C_3 vegetation regardless of water availability[47,48], and observed changes in past altitudinal distributions of these plant types have been used to document past temperature shifts and the influence on human populations[49-51]. Mean annual precipitation in Lesotho's Mesic Highveld Grassland bioregion is around 720 mm while mean annual potential evaporation can exceed 1,900 mm yearly[43]. Mean annual temperature is around 14° C, but temperature records indicate that southern Africa has experienced significant 21st century warming with an average increase of nearly 0.8 °C[52,53]. At Metolong, roughly 1.0 km from Ha Makotoko, annual precipitation can exceed 900 mm and mean annual temperature is around 17° C (Fig. S4). Therefore, past temperature shifts can be inferred by the contraction (cold shifts) or expansion (warm shifts) of the proportional C_4 contribution to sedimentary biomarkers (as interpreted through $\delta^{13}C$).

There are, however, a number of plant families that contain species which exhibit crassulacean acid metabolism (CAM) photosynthesis, in addition to combined C_3-CAM and C_4-CAM photosynthesis. Not all are necessarily known, but rather, are assumed based on other species in the same families which are found outside of Lesotho. Whilst some are classified as constitutive CAM plants, some of these species might also show some degree of plasticity in CAM expression in response to environmental conditions. For example, those in the Aizoaceae family, unlike many other succulents, do not rely solely on CAM photosynthesis, but instead, switch back and forth between C_3 and CAM, presumably to improve plant water-use efficiency. A number of succulents in the Asphodelaceae family, like *Aloe* species, use CAM photosynthesis but generally do not make up large portions of the vegetation in this part of Lesotho. With regard to $\delta^{13}C$, some CAM and most facultative CAM species[54] have overlapping values with C_3 plants in their C_{29}-C_{33} *n*-alkanes, which therefore causes issues with understanding ecosystem scale C_3-C_4 proportions. Nevertheless, seeing as Ha Makotoko is located in the Mesic Highveld Grassland bioregion, which is dominated by grasses, who do not think our precipitation and temperature change interpretations are misguided and that the overall contribution of CAM plants is minimal. This is also confirmed by phytolith work in the region[46,51].

The perceived power of isotope analyses in Lesotho is currently based on bulk $\delta^{13}C$ measured on grasses from four altitudinal transects between 1,600 and 2,600 m a.s.l. in 1994/5[50], and assumptions coming from fluctuations seen in palaeoenvironmental records of soil organic matter and mammalian tooth enamel[46,49,51,55]. There is currently no reference of bulk soil organic matter (SOM), nor have compound specific *n*-alkane $\delta^{13}C$ measurements been undertaken in the region.

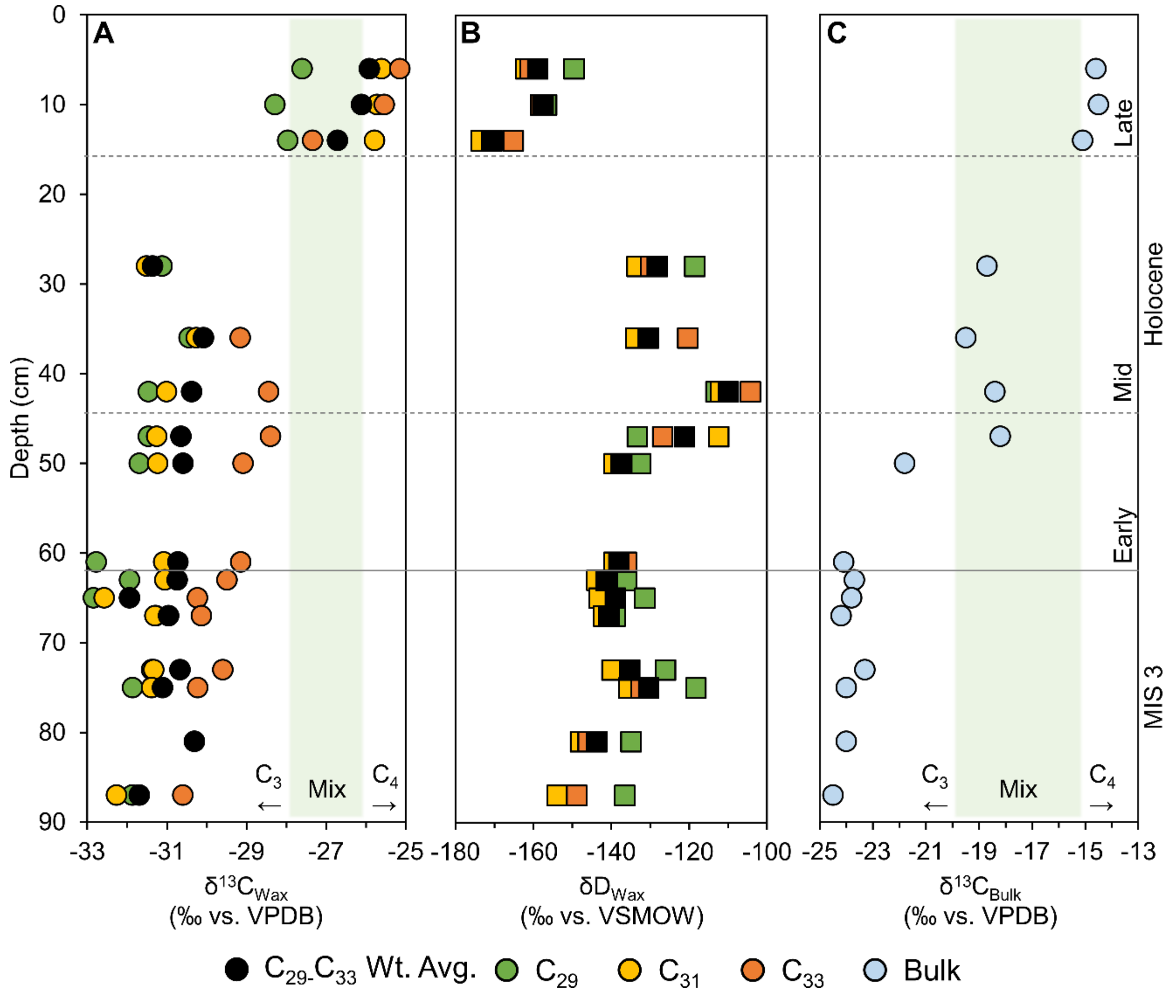

Fig. S1. Compound-specific and bulk isotope values from Ha Makotoko. (*A*) Plant wax $\delta^{13}C$ values of the individual C_{29}-C_{33} *n*-alkanes and the weighted average. (*B*) Plant wax δD values of the individual C_{29}-C_{33} *n*-alkanes and the weighted average. (C) Bulk sedimentary organic matter $\delta^{13}C$ (Reference 14 in main manuscript).

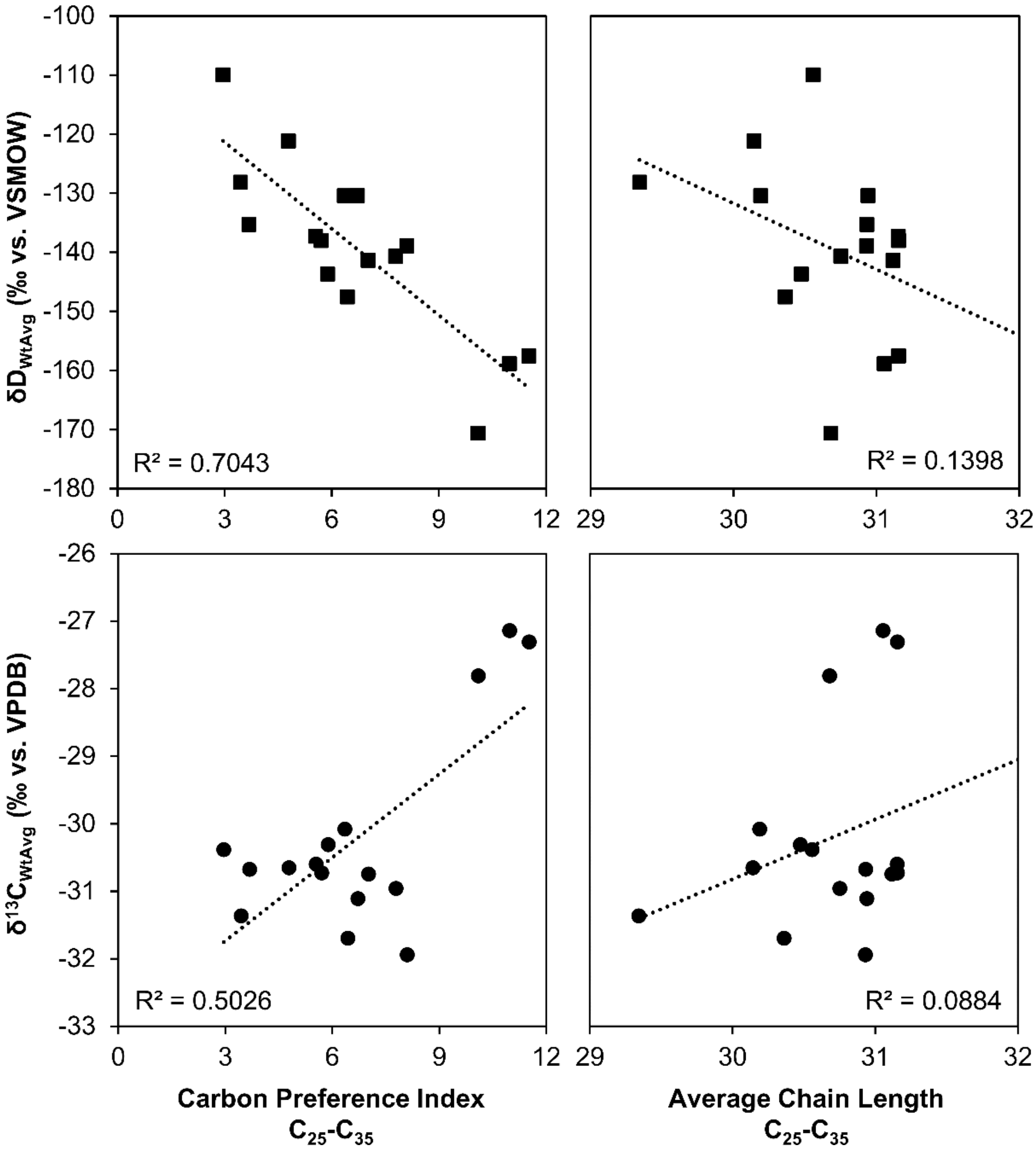

Fig. S2. Correlation between carbon and hydrogen isotopes and CPI and ACL. C_{29}-C_{33} weighted average δD and $\delta^{13}C$ versus carbon preference index (CPI) and average chain length (ACL) of the C_{25}-C_{35} *n*-alkanes. Linear correlation (R^2 on plots) and the Spearman's correlation (r_s = -0.804, p = <0.001. See Table 1 in Main Manuscript), between δD and CPI is interesting and needs to be investigated further.

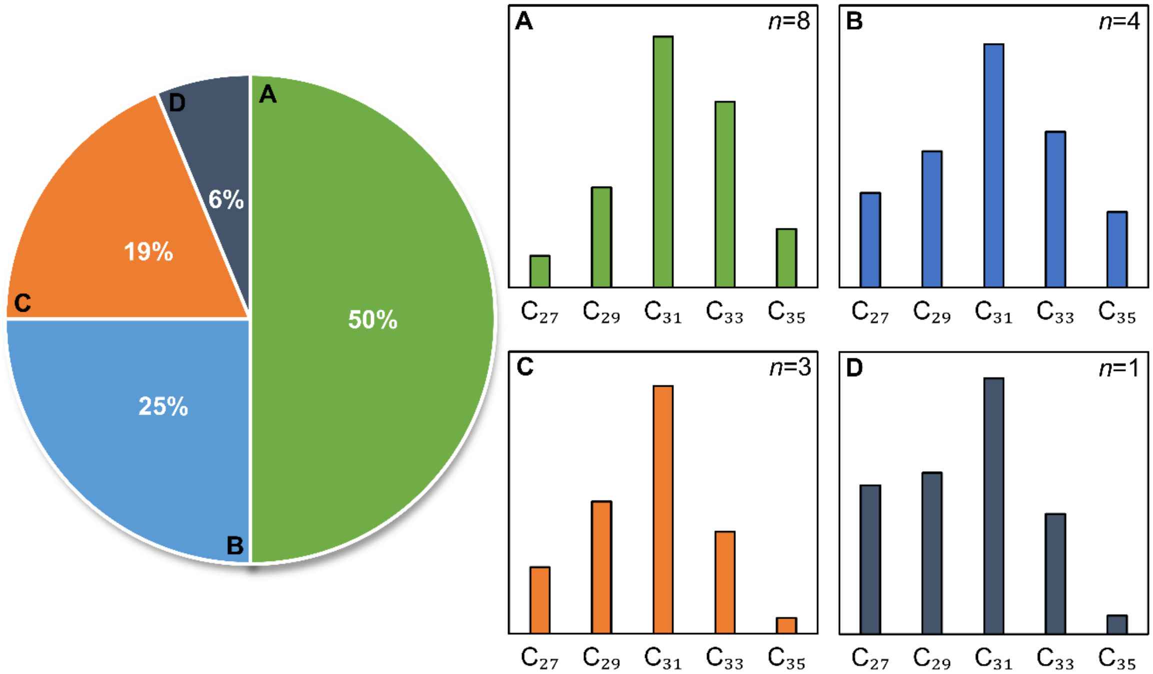

Fig. S3. Plant wax *n*-alkane compound distributions for the 16 Ha Makotoko samples. C_{31} is the dominant compound in all samples. (*A*) Eight samples (50 %) have a C_{31}, C_{33}, C_{29}, C_{35}, and C_{27} distribution; (*B*) four (25 %) have C_{31} followed by C_{33}, C_{29}, C_{27}, and C_{35}; (*C*) three (19 %) have C_{31} then C_{29}, C_{33}, C_{27}, and C_{35}; and (*D*) one (6 %) sample has a distribution of C_{31}, C_{29}, C_{27}, C_{33}, and C_{35}. Distributions may represent differences in plant ecology.

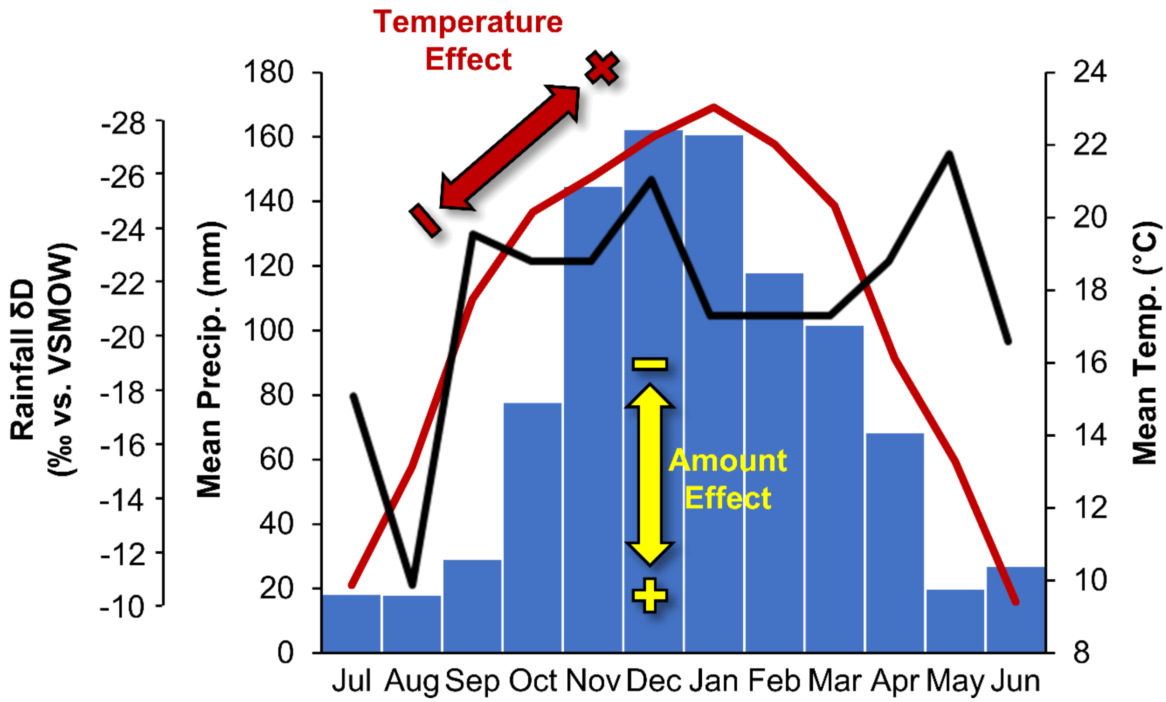

Fig. S4. Modern climate parameters of Ha Makotoko. Average monthly precipitation and temperature of Metolong, Lesotho, and δD estimations of precipitation from the Online Isotopes in Precipitation calculator (OIPC[56]) for Ha Makotoko (-29.3258°, 27.8047°, 1,640 m.a.s.l.). Both precipitation amount and temperature influence precipitation and plant wax δD, but in opposite directions. While increased precipitation lowers δD, increased temperature raises δD. Lesotho does not have a Global Network of Isotopes in Precipitation (GNIP) station, nor have modern calibration studies using precipitation or plant wax δD been performed, so caution must be taken with using precipitation δD values from the OIPC.

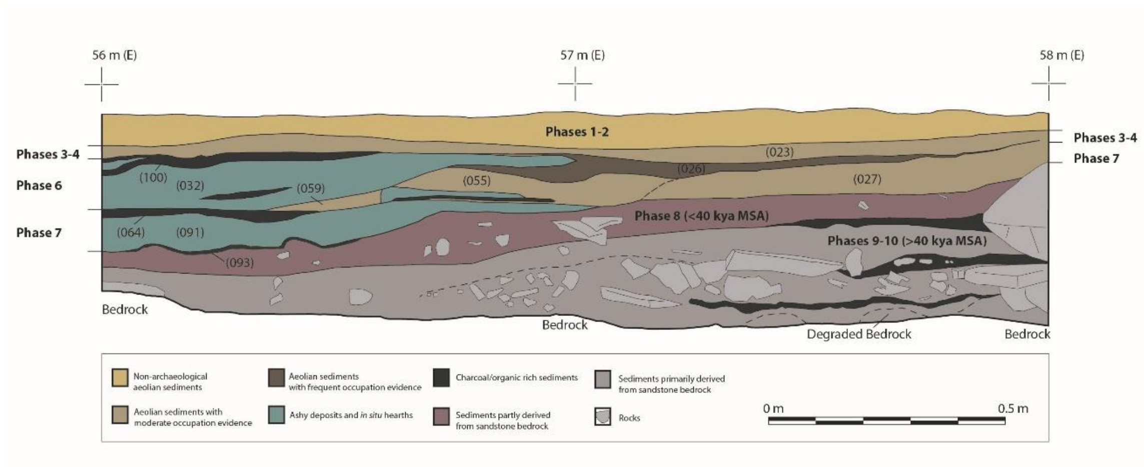

Fig. S5. Ha Makotoko stratigraphic profile. Profile is of the main excavation trench (see references 17, 27, and 53 in main manuscript for full description of the site and the archaeological excavations). Samples analyzed in this study came from an adjacent geoarchaeological column that had direct stratigraphic relationships to those in the open excavation area. Additional samples (*n*=5), however, were taken as loose sediment during excavation from Ha Makotoko's main trench and used for bulk carbon isotope analyses (see reference 14 in main manuscript).

Table S1. Tie-point samples of the 6 radiocarbon-dated layers and "modern" top layer.

Sample ID	^{14}C Age	StDev	Context No.	Depth	Thickness	Curve
NA	0	30	5	0.03	0.06	Normal
UGAMS-8984	9110	30	23	0.5	0.01	shcal20
UGAMS-8985	9320	30	32	0.55	0.01	shcal20
UGAMS-8986	10060	30	136	0.62	0.01	shcal20
UGAMS-8987	9870	30	93	0.62	0.01	shcal20
UGAMS-8988	40100	230	60	0.66	0.01	shcal20

Extended Data (separate file). Interpolated ages, biomarker metrices, and carbon and hydrogen isotope values and standard error of the mean are presented for each sample.

Replication for Age-Depth Model of Ha Makotoko

Load Necessary Libraries and Data

```
library(Bchron)
library(ggplot2)
library(ggrepel)

hm_data <- read.csv("../Data/HM_age_depth_isotopes.csv")

hm_data_bchron <- read.csv("../Data/HM_age_depth_bchron.csv")[-c(6),]

sample_depths <- hm_data$depth_m
sample_depths <- sample_depths[!is.na(sample_depths)]
interp_depth_range <- range(sample_depths)
interp_depths <- seq(0,
                     interp_depth_range[2],
                     0.01)
```

Run Bchronology

```
hm_agedepth <- Bchronology(ages = hm_data_bchron$c14age,
                           ageSds = hm_data_bchron$sd,
                           positions = hm_data_bchron$depth,
                           positionThicknesses = hm_data_bchron$thickness,
                           calCurves = hm_data_bchron$curve,
                           predictPositions = interp_depths,
                           extractDate = 1950 - 2009)
```

Summarize the model

```
hm_agedepth_mean <- apply(hm_agedepth$thetaPredict,
                          2,
                          mean)

hm_agedepth_quant <- t(apply(hm_agedepth$thetaPredict,
                             2,
                             quantile,
                             probs = c(0.05, 0.95)))
```

```
hm_agedepth_summary <- data.frame(Depth_m = interp_depths,
                                  Mean_YBP = hm_agedepth_mean,
                                  L05 = hm_agedepth_quant[, 1],
                                  U95 = hm_agedepth_quant[, 2])

hm_agedepth_summary_sample <- subset(hm_agedepth_summary,
                                  Depth_m %in% sample_depths)
```

Write out results

```
write.table(hm_agedepth_summary,
            file = "../Output/hm_agedepth_Bchron.csv",
            sep = ",",
            row.names = F)

write.table(hm_agedepth_summary_sample,
            file = "../Output/hm_agedepth_Bchron_sample.csv",
            sep = ",",
            row.names = F)

hm_data_with_agedepth <- merge(hm_data,
                            hm_agedepth_summary_sample,
                            by.x = 5,
                            by.y = 1)

write.table(hm_data_with_agedepth,
            file = "../Output/hm_agedepth_Bchron_sample_merged.csv",
            sep = ",",
            row.names = F)
```

Plot the model

```
ggplot(hm_agedepth_summary) +
    geom_ribbon(mapping = aes(xmin = L05, xmax = U95, y = Depth_m),
                fill = "steelblue") +
    geom_line(mapping = aes(y = Depth_m, x = Mean_YBP)) +
    geom_point(data = hm_agedepth_summary_sample,
            mapping = aes(y = Depth_m, x = Mean_YBP)) +
    geom_text_repel(data = hm_agedepth_summary_sample,
            mapping = aes(y = Depth_m, x = Mean_YBP, label = Depth_m),
            nudge_x = 2000) +
    labs(x = "Year BP",
        y = "Depth (m)") +
    scale_y_reverse() +
    scale_x_reverse() +
    theme_minimal()
```

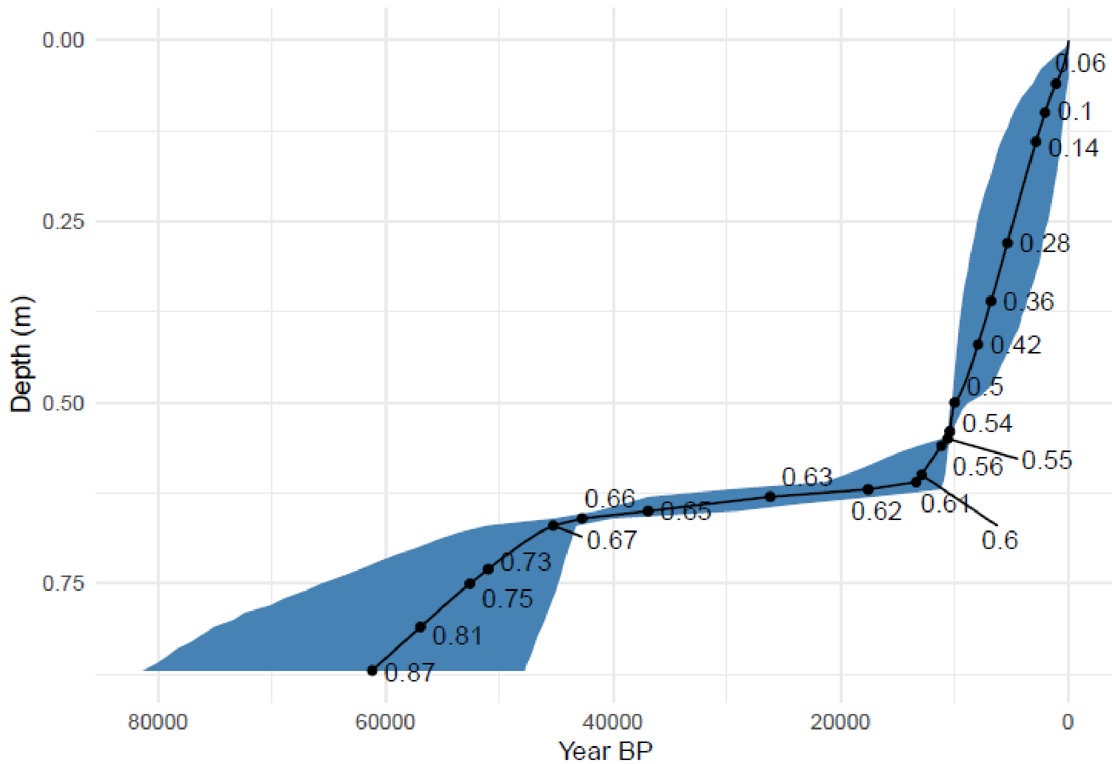


```
ggsave(device = "pdf",
    file = "../Output/agedepth_Bchron.pdf")
```

```
## Saving 6.5 x 4.5 in image
```

Fig. S6. Age-depth model. Plot of the age-depth model that includes upper and lower uncertainty estimates based on the 5-95 % quantile ranges for interpolated ages. The plot was also produced in R with ggplot2[57]. The R code and data used to produce the age-depth model can be found on Github (https://github.com/wccarleton/hm_agedepth).

SI References

1 Castañeda, I. S. & Schouten, S. A review of molecular organic proxies for examining modern and ancient lacustrine environments. *Quaternary Science Reviews* **30**, 2845-2891 (2011).
2 Eglinton, T. I. & Eglinton, G. Molecular Proxies for Paleoclimatology. *Earth and Planetary Science Letters* **275**, 1-16 (2008).
3 Cranwell, P. A., Eglinton, G. & Robinson, N. Lipids of aquatic organisms as potential contributors to lacustrine sediments. *Organic Geochemistry* **11**, 513-527 (1987).
4 Cranwell, P. A. Lipid geochemistry of sediments from Upton Broad, a small productive lake. *Organic Geochemistry* **7**, 25-37 (1984).
5 Ficken, K. J., Li, B., Swain, D. L. & Eglinton, G. An *n*-alkane proxy for the sedimentary input of submerged/floating freshwater aquatic macrophytes. *Organic Geochemistry* **31**, 745-749 (2000).
6 Barnes, M. A. & Barnes, W. C. in *Lakes: Chemistry, Geology, Physics* (ed A. Lerman) 127-152 (Springer-Verlag, 1978).
7 Eglinton, G. & Hamilton, R. J. Leaf epicuticular waxes. *Science* **156**, 1322-1335 (1967).
8 Bush, R. T. & McInerney, F. A. Leaf wax *n*-alkane distributions in and across modern plants: Implications for paleoecology and chemotaxonomy. *Geochimica et Cosmochimica Acta* **117**, 161-179 (2013).
9 Tipple, B. J. & Pagani, M. Environmental control on eastern broadleaf forest species' leaf wax distributions and D/H ratios. *Geochimica et Cosmochimica Acta* **111**, 64-77 (2013).
10 Bush, R. T. & McInerney, F. A. Influence of temperature and C_4 abundance on *n*-alkane chain length distributions across the central USA. *Organic Geochemistry* **79**, 65-73 (2015).
11 Castañeda, I. S., Werne, J. P., Johnson, T. C. & Filley, T. R. Late Quaternary vegetation history of southeast Africa: The molecular isotopic record from Lake Malawi. *Palaeogeography, Palaeoclimatology, Palaeoecology* **275**, 100-112, doi:https://doi.org/10.1016/j.palaeo.2009.02.008 (2009).
12 Dodd, R. S. & Poveda, M. M. Environmental gradients and population divergence contribute to variation in cuticular wax composition in *Juniperus communis*. *Biochemical Systematics and Ecology* **31**, 1257-1270, doi:https://doi.org/10.1016/S0305-1978(03)00031-0 (2003).
13 Carr, A. S. *et al.* Leaf wax *n*-alkane distributions in arid zone South African flora: Environmental controls, chemotaxonomy and palaeoecological implications. *Organic Geochemistry* **67**, 72-84, doi:https://doi.org/10.1016/j.orggeochem.2013.12.004 (2014).
14 Sachse, D., Radke, J. & Gleixner, G. δD values of individual *n*-alkanes from terrestrial plants along a climatic gradient – Implications for the sedimentary biomarker record. *Organic Geochemistry* **37**, 469-483 (2006).
15 O'Leary, M. Carbon Isotope Fractionation in Plants. *Phytochemistry* **20**, 553-567 (1981).

16 Yang, H. *et al.* Carbon and hydrogen isotope fractionation under continuous light: implications for paleoenvironmental interpretations of the High Arctic during Paleogene warming. *Oecologia* **160**, 461-470 (2009).
17 Suh, Y. J. & Diefendorf, A. F. Seasonal and canopy height variation in *n*-alkanes and their carbon isotopes in a temperate forest. *Organic Geochemistry* **116**, 23-34, doi:https://doi.org/10.1016/j.orggeochem.2017.10.015 (2018).
18 Chikaraishi, Y. & Naraoka, H. Compound-specific δD-$\delta^{13}C$ analyses of *n*-alkanes extracted from terrestrial and aquatic plants. *Phytochemistry* **63**, 361-371 (2003).
19 Schubert, B. A. & Jahren, A. H. Global increase in plant carbon isotope fractionation following the Last Glacial Maximum caused by increase in atmospheric *p*CO2. *Geology* **43**, 435-438 (2015).
20 Ehleringer, J. R. in *Stable Isotopes in Ecological Research* Vol. 68 *Ecological Studies* (eds P. W. Rundel, J. R. Ehleringer, & K. A. Nagy) Ch. 3, 525 (Springer-Verlag, 1989).
21 Farquhar, G. D., Hubick, K. T., Condon, A. G. & Richards, R. A. in *Stable Isotopes in Ecological Research* Vol. 68 *Ecological Studies* (eds P. W. Rundel, J. R. Ehleringer, & K. A. Nagy) Ch. 21, 525 (Springer-Verlag, 1989).
22 Collister, J. W., Rieley, G., Stern, B., Eglinton, G. & Fry, B. Compound-specific $\delta^{13}C$ analyses of leaf lipids from plants with differing carbon dioxide metabolims. *Organic Geochemistry* **21**, 619-627 (1994).
23 Rommerskirchen, F., Plader, A., Eglinton, G., Chikaraishi, Y. & Rullkötter, J. Chemotaxonomic significance of distribution and stable carbon isotopic composition of long-chain alkanes and alkan-1-ols in C_4 grass waxes. *Organic Geochemistry* **37**, 1303-1332 (2006).
24 Vogts, A., Moossen, H., Rommerskirchen, F. & Rullkötter, J. Distribution patterns and stable carbon isotopic composition of alkanes and alkan-1-ols from plant waxes of African rain forest and savanna C_3 species. *Organic Geochemistry* **40**, 1037-1054 (2009).
25 Bi, X., Sheng, G., Liu, X., Li, C. & Fu, J. Molecular and carbon and hydrogen isotopic composition of *n*-alkanes in plant leaf waxes. *Organic Geochemistry* **36**, 1405-1417 (2005).
26 Kristen, I. *et al.* Biomarker and stable carbon isotope analyses of sedimentary organic matter from Lake Tswaing: evidence for deglacial wetness and early Holocene drought from South Africa. *Journal of Paleolimnology* **44**, 143-160, doi:10.1007/s10933-009-9393-9 (2010).
27 Esteban, I. *et al.* Coastal palaeoenvironments and hunter-gatherer plant-use at Waterfall Bluff rock shelter in Mpondoland (South Africa) from MIS 3 to the Early Holocene. *Quaternary Science Reviews* **250**, 106664, doi:https://doi.org/10.1016/j.quascirev.2020.106664 (2020).
28 Hou, J., D'Andrea, W. J., MacDonald, D. & Huang, Y. Evidence for water use efficiency as an important factor in determining the δD values of tree leaf waxes. *Organic Geochemistry* **38**, 1251-1255 (2007).
29 Huang, Y. *et al.* Climatic and environmental controls on the variation of C_3 and C_4 plant abundances in central Florida for the past 62,000 years. *Palaeogeography, Palaeoclimatology, Palaeoecology* **237**, 428-435 (2006).

30 Smith, F. A. & Freeman, K. H. Influence of physiology and climate on δD of leaf wax *n*-alkanes from C_3 and C_4 grasses. *Geochimica et Cosmochimica Acta* **70**, 1172-1187 (2006).
31 Chikaraishi, Y. & Naraoka, H. $\delta^{13}C$ and δD relationships among three *n*-alkyl compound classes (*n*-alkanoic acid, *n*-alkane and *n*-alkanol) of terrestrial higher plants. *Organic Geochemistry* **38**, 198-215 (2007).
32 Garcin, Y. *et al.* Hydrogen isotope ratios of lacustrine sedimentary *n*-alkanes as proxies of tropical African hydrology: insights from a calibration transect across Cameroon. *Geochimica et Cosmochimica Acta* **79**, 106-126 (2012).
33 Hou, J., D'Andrea, W. J., MacDonald, D. & Huang, Y. Hydrogen isotopic variability in leaf waxes among terrestrial and aquatic plants around Blood Pond, Massachusetts (USA). *Organic Geochemistry* **38**, 977-984, doi:10.1016/j.orggeochem.2006.12.009 (2007).
34 Sachse, D., Radke, J. & Gleixner, G. Hydrogen isotope ratios of recent lacustrine sedimentary *n*-alkanes record modern climate variability. *Geochim Cosmochim Acta* **68**, 4877-4889 (2004).
35 Sauer, P., Eglinton, T. I., Hayes, J. M., Schimmelmann, A. & Sessions, A. L. Compound-specific D/H ratios of lipid biomarkers from sediments as a proxy for environmental and climatic conditions. *Geochim Cosmochim Acta* **65**, 213-222 (2001).
36 Huang, Y., Shuman, B., Wang, Y. & III., W. T. Hydrogen isotope ratios of individual lipids in lake sediments as novel tracers of climatic and environmental change: a surface sediment test. *Journal of Paleoclimatology* **31**, 363-375 (2004).
37 Sessions, A. L., Burgoyne, T. W., Schimmelmann, A. & Hayes, J. M. Fractionation of hydrogen isotopes in lipid biosynthesis. *Organic Geochemistry* **30**, 1193-1200 (1999).
38 Sachse, D. *et al.* Molecular Paleohydrology, Interpreting the Hydrogen-Isotopic Composition of Lipid Biomarkers from Photosynthesizing Organisms. *Annual Review of Earth and Planetary Sciences* **40**, 221-249, doi:10.1146/annurev-earth-042711-105535 (2012).
39 Dansgaard, W. Stable isotopes in precipitation. *Tellus* **16**, 436-468 (1964).
40 Hermann, N. *et al.* Hydrogen isotope fractionation of leaf wax *n*-alkanes in southern African soils. *Organic Geochemistry* **109**, 1-13 (2017).
41 Ehleringer, J. R., Cerling, T. E. & Helliker, B. R. C_4 photosynthesis, atmospheric CO_2, and climate. *Oecologia* **112**, 285-299, doi:10.1007/s004420050311 (1997).
42 Tipple, B. J. & Pagani, M. The Early Origins of Terrestrial C_4 Photosynthesis. *Annual Review of Earth and Planetary Sciences* **35**, 435-461 (2007).
43 Mucina, L. & Rutherford, M. in *Strelitzia* Vol. 19 (Sanbi, Pretoria, 2006).
44 Guillarmod, J. A. *Flora of Lesotho (Basutoland)*. 474 (Verlag Von Cramer, 1971).
45 Werger, M. J. A. *Biogeography and Ecology of Southern Africa*. Vol. 1 (W. Junk, 1978).
46 Parker, A. G., Lee-Thorp, J. & Mitchell, P. J. Late Holocene Neoglacial conditions from the Lesotho highlands, southern Africa: phytolith and stable carbon isotope evidence from the archaeological site of Likoaeng. *Proceedings of the Geologists' Association* **122**, 201-211, doi:https://doi.org/10.1016/j.pgeola.2010.09.005 (2011).
47 Tieszen, L. L., Senyimba, M. M., Imbamba, S. K. & Troughton, J. H. The distribution of C3 and C4 grasses and carbon isotope discrimination along an altitudinal and

moisture gradient in Kenya. *Oecologia* **37**, 337-350, doi:10.1007/BF00347910 (1979).
48 Livingstone, D. A. & Clayton, W. D. An altitudinal cline in tropical African grass floras and its paleoecological significance. *Quaternary Research* **13**, 392-402, doi:https://doi.org/10.1016/0033-5894(80)90065-4 (1980).
49 Roberts, P., Lee-Thorp, J. A., Mitchell, P. J. & Arthur, C. Stable carbon isotopic evidence for climate change across the late Pleistocene to early Holocene from Lesotho, southern Africa. *Journal of Quaternary Science* **28**, 360-369, doi:https://doi.org/10.1002/jqs.2624 (2013).
50 Smith, J. M., Lee-Thorp, J. A. & Sealy, J. Stable carbon and oxygen isotopic evidence for late Pleistocene to middle Holocene climatic fluctuations in the interior of southern Africa. *Journal of Quaternary Science* **17**, 683-695 (2002).
51 Stewart, B. A., Parker, A. G., Dewar, G., Morley, M. W. & Allott, L. F. in *Africa from MIS 6-2: Population Dynamics and Paleoenvironments* (eds Sacha C. Jones & Brian A. Stewart) 247-271 (Springer Netherlands, 2016).
52 Bank, W. Lesotho Water Security and Climate Change Assessment. (World Bank, Washington, DC, 2016).
53 Niang, I. *et al.* in *Climate Impacts, Adaptation, and Vulnerability. Part B: Regional Aspects. Contribution of Working Group II to the Fifth Assessment Report of the Intergovernmental Panel on Climate Change* (eds V. R. Barros *et al.*) Ch. 22, 1199-1265 (Cambridge University Press, 2014).
54 Boom, A., Carr, A. S., Chase, B. M., Grimes, H. L. & Meadows, M. E. Leaf wax n-alkanes and δ13C values of CAM plants from arid southwest Africa. *Organic Geochemistry* **67**, 99-102, doi:https://doi.org/10.1016/j.orggeochem.2013.12.005 (2014).
55 Loftus, E., Stewart, B. A., Dewar, G. & Lee-Thorp, J. Stable isotope evidence of late MIS 3 to middle Holocene palaeoenvironments from Sehonghong Rockshelter, eastern Lesotho. *Journal of Quaternary Science* **30**, 805-816, doi:https://doi.org/10.1002/jqs.2817 (2015).
56 Bowen, G. J. & Revenaugh, J. Interpolating the isotopic composition of modern meteoric precipitation. *Water Resources Research* **39**, doi:10.129/2003WR002086 (2003).
57 Wickham, H. *Ggplot2: Elegant Graphics for Data Analysis*, <https://ggplot2.tidyverse.org> (2016).